Effect of Co and O defects on the magnetism in Co-doped ZnO: Experiment and theory

G. S. Chang,[1,*] E. Z. Kurmaev,[2] D. W. Boukhvalov,[3] L. D. Finkelstein,[2] S. Colis,[4] T. M. Pedersen,[1] A. Moewes,[1] and A. Dinia[4]

[1]*Department of Physics and Engineering Physics, University of Saskatchewan, 116 Science Place, Saskatoon, SK, Canada S7N 5E2*

[2]*Institute of Metal Physics, Russian Academy of Sciences–Ural Division, 620041 Yekaterinburg, Russia*

[3]*Institute for Molecules and Materials, Radboud University, NL-6525 ED Nijmegen, The Netherlands*

[4]*IPCMS CNRS-UMR 7504, ULP-ECPM, 23 Rue du Loess, F-67034 Strasbourg, France*

(Received 9 November 2006; revised manuscript received 12 February 2007; published 29 May 2007)

The electronic structure of $Zn_{1-x}Co_xO$ (x=0.02, 0.06, and 0.10) diluted magnetic semiconductors is investigated using soft x-ray emission spectroscopy and first-principles calculations. X-ray absorption and emission measurements reveal that most Co dopants are incorporated at the Zn sites and that free charge carriers are absent over a wide range of Co concentrations. The excess Co interstitials appear in the samples with high Co concentration (10 at. %) but are isolated without any direct exchange interaction with substitutional Co atoms. The lack of free charge carriers and the direct Co-Co interactions is responsible for the absence of ferromagnetism in the samples. First-principles calculations suggest that the exchange interaction between substitutional Co atoms induces only an antiferromagnetic coupling, and strong ferromagnetism in Co-doped ZnO requires not only free charge carriers but also the Co interstitials directly interacting with substitutional Co atoms.

DOI: 10.1103/PhysRevB.75.195215 PACS number(s): 78.70.En, 75.50.Pp, 71.20.Nr, 75.30.Hx

I. INTRODUCTION

Transition metal-doped ZnO has garnered special interest as diluted magnetic semiconductor (DMS) material, because ZnO as a host material is piezoelectric and optically transparent with a wide band gap of 3.3 eV and a large exciton binding energy of 60 meV.[1] For ZnO-based DMS systems, the existence of ferromagnetic ordering in Co-doped ZnO was predicted theoretically on the basis of the double-exchange interaction between Co ions.[2] The Ruderman-Kittel-Kasuya-Yosida (RKKY) interaction was later suggested as the origin of ferromagnetism by Jalbout *et al.*[3] In view of the experimental approaches, enormous research efforts have been directed toward realizing ferromagnetic ZnO:Co with high Curie temperature (T_C). Ueda *et al.* reported ferromagnetic behavior of ZnO:Co films synthesized by pulsed-laser deposition and with a T_C above 300 K.[4] Subsequent experiments showed that magnetic moments of $Zn_{1-x}Co_xO$ films grown by various techniques spread over a relatively wide range from 0.56 to 2.6 μ_B/Co.[5] On the other hand, Jin *et al.* claimed no trace of ferromagnetism in films grown by laser molecular-beam epitaxy.[6]

More recently, the formation of Co-metal clusters has been considered as a possible origin for ferromagnetism. Norton *et al.* suggested the formation of (110)-oriented hexagonal phase Co nanocrystals in the Co-implanted ZnO samples although the diameter of their Co nanocrystals (3.6 nm) was below the superparamagnetic critical size for Co.[7] This array of seemingly contradicting experimental results as well as some lack of reproducibility has hampered practical applications of this system to electronic technology. In order to understand the inconsistencies in experimental results and to shed light on the possible presence (or absence) of ferromagnetism in the ZnO:Co system, information on the local electronic structure near the magnetic impurities is essential because magnetic properties of the ZnO:Co systems have been known to be strongly correlated with exchange interaction mediated by charge carriers and direct double-exchange mechanism between magnetic ions.

In this paper, we employ resonant inelastic x-ray scattering (RIXS) to extensively investigate the electronic structure of Co, Zn, and O in $Zn_{1-x}Co_xO$ (x=0.02, 0.05, and 0.10) samples. First-principles calculations are performed for various model clusters with different types of Co and O defects and are compared to the spectroscopic measurements. Our results suggest that the presence of free charge carriers is necessary but not sufficient for any ferromagnetic ordering in the $Zn_{1-x}Co_xO$ system even though Co dopants are incorporated at the Zn sites. Strong ferromagnetism also requires the interstitial Co atoms interacting with the adjacent Co substitutional atoms.

II. EXPERIMENTAL

The oxalate precursor $Zn_{1-x}Co_x(C_2O_4)2H_2O$ was obtained by coprecipitation of 50 ml of a 0.4 mol/l aqueous solution of Zn and Co acetates [$Zn(OAc)_2$, $2H_2O$, and $Co(OAc)_2$, $4H_2O$, respectively] with the same volume of a 0.4 mol/l solution of oxalic acid at room temperature (RT). The as-prepared $Zn_{1-x}Co_xO$ powders were then heated at 1173 K for 15 min in air. The removal of all traces of C and H is confirmed using thermogravimetric analysis and x-ray photoelectron spectroscopy. X-ray diffraction and transmission electron microscopy measurements of the $Zn_{1-x}Co_xO$ powders with Co concentrations of x=2, 6, and 10 at. % show that all samples have a similar wurtzite phase without any secondary phase. According to Janisch *et al.*,[5] the thermal solubility limit for Co in ZnO is 10 at. % and higher but it depends on different fabrication techniques. However, the magnetization curves exhibit a feature typical for paramagnetic samples even at the lowest temperature measured (5 K). The absence of ferromagnetism in $Zn_{1-x}Co_xO$ powders prepared by a precursor-decomposition method is in agreement with other results reported.[8] Substitution of Co^{2+}

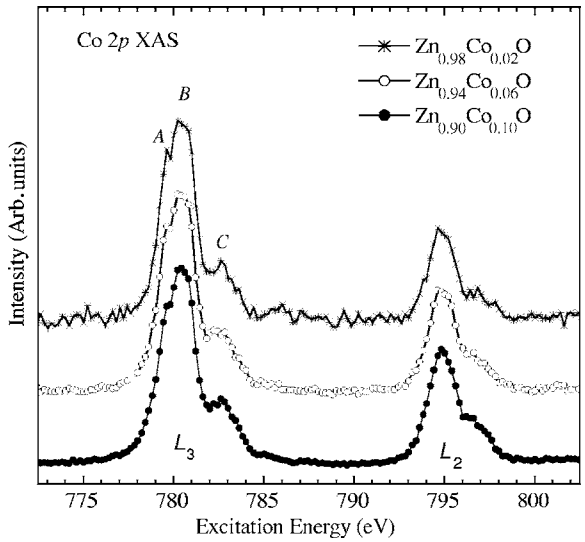

FIG. 1. Co $2p$ x-ray absorption spectra of $Zn_{1-x}Co_xO$ (x=0.02, 0.06, and 0.10). The spectra are normalized to the same peak height of the Co L_3 peak.

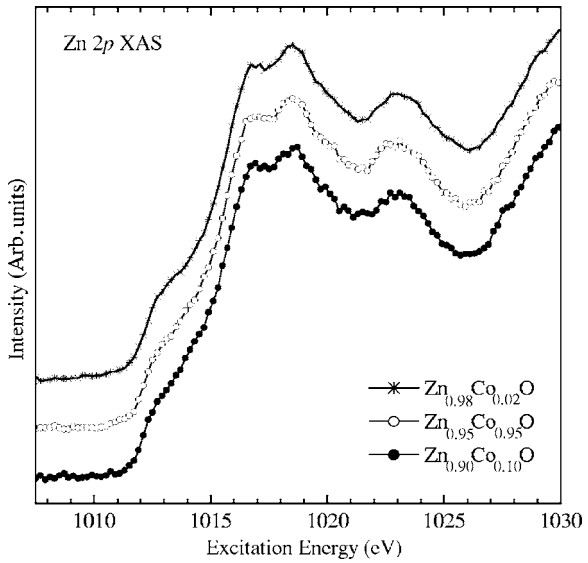

FIG. 2. Zn $2p$ x-ray absorption spectra of $Zn_{1-x}Co_xO$ (x=0.02, 0.06, and 0.10).

ions for Zn^{2+} ions is confirmed by optical reflectance measurements. In addition, the magnetic susceptibility versus temperature curves reveal that excess Co impurities are antiferromagnetically coupled through oxygen atoms. Further details on the growth and magnetic characterization of $Zn_{1-x}Co_xO$ are reported elsewhere.[9]

To elucidate the absence of ferromagnetism in $Zn_{1-x}Co_xO$ samples, x-ray absorption and emission spectroscopy were employed to study the local electronic structure of Co impurities in the samples. The measurements were carried out at Beamline 8.0.1 of the Advanced Light Source at Lawrence Berkeley National Laboratory. Co $L_{2,3}$ ($3d4s \rightarrow 2p$ transition) and Zn $L_{2,3}$ RIXS spectra were obtained using excitation energies near L_3 and L_2 absorption thresholds. On the other hand, nonresonant O $K\alpha$ ($2p \rightarrow 1s$ transition) emission spectra were measured at the excitation energy well above the absorption thresholds. All spectra were recorded at room temperature (RT). All measured spectra are normalized to the number of photons falling on the sample monitored by a highly transparent gold mesh.

III. RESULTS AND DISCUSSION

A. X-ray absorption spectra

Figure 1 shows the Co $2p$ x-ray absorption spectra (XAS) of $Zn_{1-x}Co_xO$ (x=0.02, 0.06, and 0.10), which result from $2p \rightarrow 3d$ dipole transitions. All spectra were acquired in total fluorescence-yield mode, which is more bulk sensitive than measurements in total electron-yield mode. The Co L_3 and L_2 absorption lines are located around 780 and 795 eV, respectively, and their large energy separation is due to spin-orbit splitting of the $2p$ core holes. Multiplet features resulting from Coulomb and exchange interactions of the $2p$ core holes with the $3d$ electrons (features A through C) are clearly seen in all spectra. Energy positions and intensities of multiplet features are in good agreement with previous measurements of $Zn_{1-x}Co_xO$ (x=0.011–0.054) and calculated Co $2p$ XAS spectra of a Co^{2+} ion in a tetrahedral cluster (based on the configuration-interaction cluster model).[10,11] This suggests that the majority of Co dopants reside at the Zn sites (for all Co concentrations) and that they are tetrahedrally coordinated with the ligand O atoms. Therefore the magnetic properties of the samples investigated most likely arise from the hybridization between ligand O $2p$ orbitals and localized Co $3d$ orbitals in the substitutional sites. On the other hand, the Zn $2p$ XAS spectra are not found to display any noticeable change as the Co concentration increases, as shown in Fig. 2. The overall features are very similar to that of the undoped ZnO sample[11] indicating that the Zn-related defects such as Zn interstitials or Zn-antisite defects are not induced upon doping of Co atoms into ZnO.

According to the Co $2p$ XAS spectra, Co impurity atoms are surrounded by O nearest neighbors. We can therefore expect that the O $1s$ XAS spectra of ZnO are affected by doping with Co atoms. It has been recently reported that ferromagnetic Co-doped ZnO thin films grown by pulsed laser deposition (PLD) exhibit different spectral behavior compared to those of undoped ZnO; namely a shift of the onset energy (of about 0.5 eV) and the appearance of additional spectral features near the bottom of the O $2p$ conduction band.[11] These are attributed to the presence of O vacancies (O_V) and the hybridization of Co $3d$ states with O $2p$ vacancy states, which are considered to be responsible for ferromagnetic ordering in Co-doped ZnO systems. In Fig. 3, we compare O $1s$ XAS spectra of our nonmagnetic samples with those of undoped ZnO and $Zn_{0.95}Co_{0.05}O$ thin films reported in Ref. 11. The main spectral features between 530 and 538 eV of undoped ZnO (labeled a through c) are assigned to O $2p$-Zn $4s$ hybridized states while the features d and e arise from O $2p$ states hybridized with Zn $4p$ states. In the case of Co-doped ZnO samples, the O $1s$ spectra show more spectral weight close to the conduction-band minimum (features a_1 and a_2) than undoped ZnO. According to the

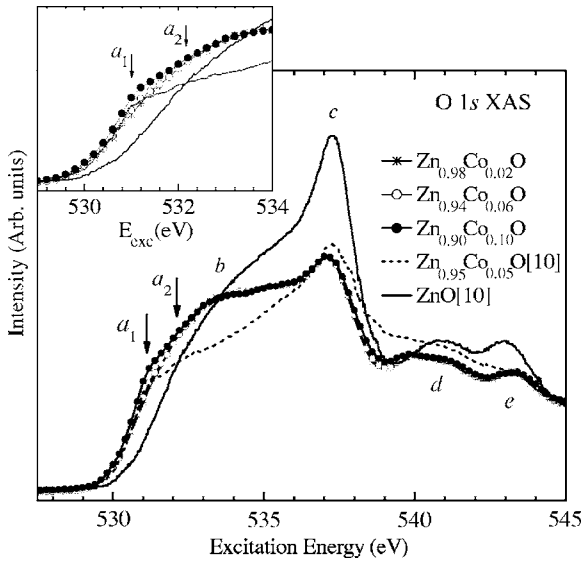

FIG. 3. O 1*s* x-ray absorption spectra of $Zn_{1-x}Co_xO$ (x=0.02, 0.06, and 0.10). The corresponding absorption spectra of $Zn_{0.95}Co_{0.05}O$ and ZnO reference samples reported in Ref. 13 are added for comparison.

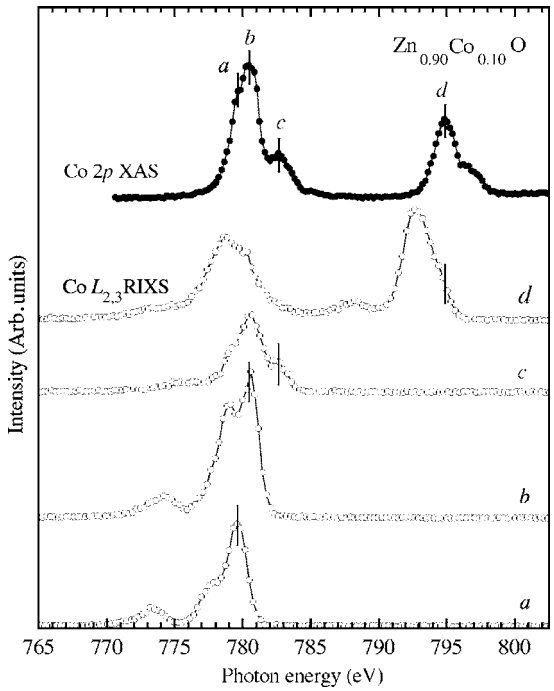

FIG. 4. Co 2*p* x-ray absorption spectrum (top) and resonantly excited Co $L_{2,3}$ x-ray emission spectra of the corresponding sample. Labels in the emission spectra indicate the corresponding excitation energies shown in the XAS spectrum.

calculations of a 32-atom wurtzite supercell of ZnO containing 1 Co atom (6.25 at. %) and 2 Co atoms (12.5 at. %) substituting for Zn-sites,[12] the majority-spin Co *d* states are fully occupied whereas the minority-spin states are partially occupied, with the Fermi level lying in the gap between the crystal field-split *e* and t_2 states. Therefore the unoccupied t_2 states can hybridize with O 2*p* states and thus are thought to be the origin of fine structures a_1 and a_2 observed in O 1*s* XAS spectra. The interesting point is that these additional features a_1 and a_2 are slightly enhanced as the Co concentration increases (see inset). This may be due to the presence of O_V defects or different Co occupancy at the interstitial sites. However, the possibility of O_V formation can be excluded from the spectral behavior of feature *b*. The spectral weight at 533.5 eV for our $Zn_{1-x}Co_xO$ samples is much higher than that for the PLD-grown $Zn_{0.95}Co_{0.05}O$ film containing O_V defects, as shown in Fig. 3. According to our first-principles calculations discussed in detail below, the presence of O_V defects only results in the reduction and broadening of feature *b* while the Co interstitials do not change this feature but enhance the a_1 and a_2 fine structures. Therefore, the different O 1*s* XAS spectra of nonmagnetic $Zn_{1-x}Co_xO$ samples from those of undoped ZnO and the O_V-containing $Zn_{0.95}Co_{0.05}O$ films seem to be caused by the Co interstitials rather than the O_V defects.

B. Co RIXS spectra

In addition to XAS spectra of constituent elements, we obtained spectral information on occupied Co 3*d* states from RIXS measurements. Since the involved x-ray transitions in the RIXS process occur within the excited atom (Co in our case) and are predominantly affected by the first coordination sphere, RIXS measurements provide an efficient way to probe local electronic structure of Co impurities. By using the RIXS technique, we can clarify whether the minority Co interstitials (estimated from the O 1*s* XAS spectra) is interacting with the majority of substitutional Co atoms or whether they exist as isolated states. Figure 4 shows the Co 2*p* XAS (top) and Co $L_{2,3}$ RIXS spectra of the $Zn_{0.90}Co_{0.10}O$. We chose four excitation energies (E_{exc}), three at L_3 (spectra labeled *a* through *c*), and one at L_2 (spectrum *d*) thresholds. The positions of the elastically scattered photons are labeled as vertical bars in the RIXS spectra. For resonant excitations at Co L_3 edge, the peaks from the intra-atomic *d*-*d* excitations are clearly shown at 777.3 and 778.8 eV in spectra *a* and *b*, respectively (about 2 eV below the elastic peak). Other broad peaks at 773.3 (in spectrum *a*) and 774.2 eV (*b*) are contributed from the charge-transfer excitations from the O ligand states to Co 3*d* states ($3d^8L$ configuration, *L* indicates a hole in the O 2*p* band). These spectral features agree fairly well with those found for CoO (100) single crystal.[13] The charge-transfer peaks of $Zn_{0.90}Co_{0.10}O$ are narrower than those in CoO, which is due to different crystal-field interactions of tetrahedrally coordinated Co^{2+} ions with the O ligand atoms from those in CoO with octahedral symmetry.

On the other hand, when the excitation energy is tuned to L_2 threshold (spectrum *d*), the intense L_2 emission line is significantly enhanced with respect to the L_3 emission. According to our previous studies,[14,15] the intensity ratio of L_2 to L_3 emission lines, $I(L_2)/I(L_3)$, is strongly affected by the amount of free carriers around the target element (Co in our case). In Fig. 5, Co $L_{2,3}$ RIXS spectra of our $Zn_{1-x}Co_xO$ (x=0.02, 0.06, and 0.10) samples are resonantly excited at L_2 threshold and compared to those of CoO and Co metal. The intensity ratio $I(L_2)/I(L_3)$ of metallic Co is much smaller

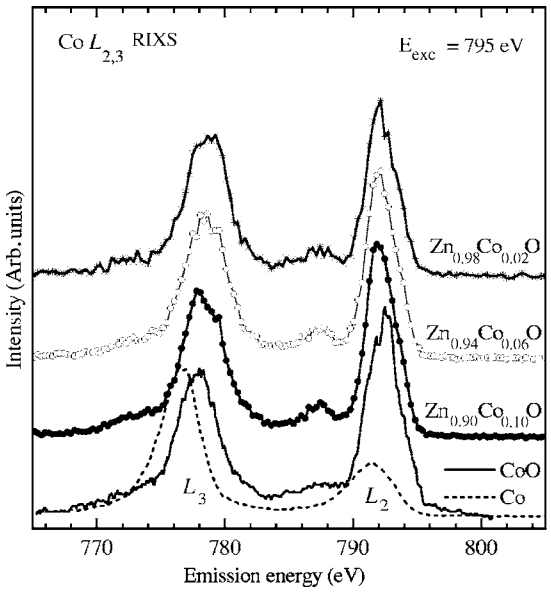

FIG. 5. Co $L_{2,3}$ RIXS spectra of $Zn_{1-x}Co_xO$ (x=0.02, 0.06, and 0.10), Co metal, and CoO samples resonantly excited at the Co L_2 edge.

than for insulating CoO. The reduction of L_2 states in metallic Co arises from radiationless $L_2L_3M_{4,5}$ Coster-Kronig (CK) transitions. These transitions of holes from the L_2 to L_3 level are competing with the normal emission process and partially depopulate the L_2 states of solids.[16] Since the CK transition energy can be released via emission of 3d Auger electrons, the effect of CK transitions is more prominent in 3d metals than in insulating (and 3d-electron depleted) oxides. Thus the $I(L_2)/I(L_3)$ ratio provides an efficient way of characterizing the variation in charge carriers and metallicity of solids. We also see in Fig. 5 that the $I(L_2)/I(L_3)$ ratio of the $Zn_{1-x}Co_xO$ samples does not change with Co concentration, and its value ($\sim$1.27) is practically similar with that of CoO and much higher than for pure Co metal ($\sim$0.62).[14] Based on the Co $L_{2,3}$ RIXS measurements, we conclude that free charge carriers—which are known to be responsible for mediating an exchange interaction between Co ions—are absent in our $Zn_{1-x}Co_xO$ samples (as in CoO) and no evidence for direct Co-Co interactions is found.

C. Electronic structure calculations

Although our spectroscopic results provide meaningful information about the local environment around the magnetic Co impurities as well as the free charge carriers, two questions still remain concerning the Co-doped ZnO system. (i) Why are free charge carriers absent in this system, and (ii) is it possible to induce ferromagnetism in Co-doped ZnO DMSs only in the presence of free charge carriers?

In order to address the above questions and comprehensively understand the spectral behavior of the system, we calculated the electronic structure of $Zn_{1-x}Co_xO$ with different defect configurations using the linearized muffin-tin-orbital method in the atomic-spheres approximation (LMTO-ASA) within the local spin-density approach (LSDA).[14,17]

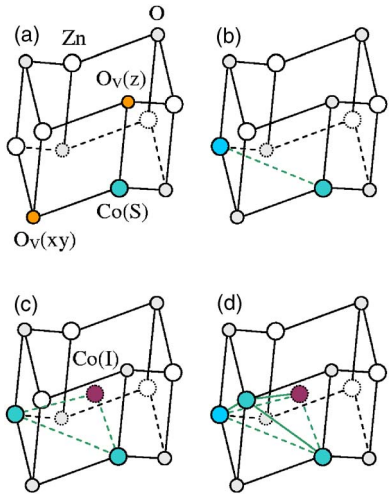

FIG. 6. (Color online) Various defect configurations in the ZnO wurtzite structure: (a) one Co(S) and two different nearest O_v defects, (b) two Co(S) atoms, (c) one Co(S) and two Co(I) atoms, and (d) three Co(S) and one Co(I) atoms.

Supercell geometry with 64 atoms in the cell ($4a\times4a\times4c$) was employed. Figure 6 depicts the model clusters with various defect configurations. First we calculated the unoccupied O 2p partial density of states (PDOS) of the clusters containing Co atoms that are substituting Zn sites [Co(S)], Co interstitials [Co(I)], and O vacancies (O_V). Figure 7(a) shows the unoccupied O 2p PDOS calculated for the clusters containing single Co(S) (solid line) and one Co(S) combined with one O_V (dashed and dotted lines). We considered two types of O_V near the Co(S) and both are depicted in

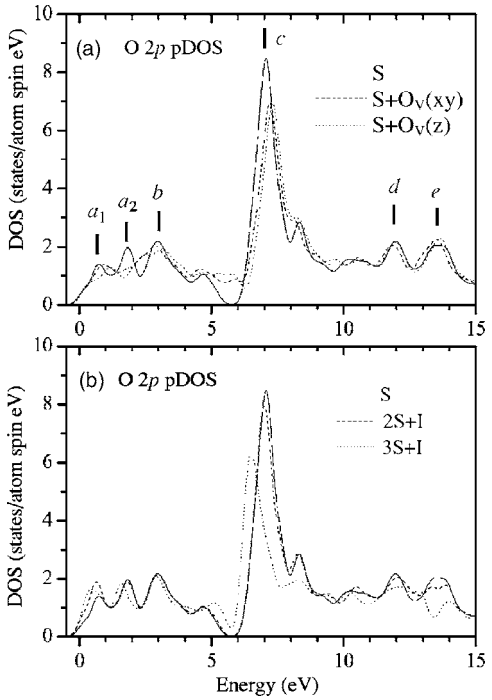

FIG. 7. Calculated unoccupied O 2p DOS: (a) for the model clusters with Co(S) and O_v defects, and (b) for the clusters with Co(S) and Co(I) defects.

TABLE I. Calculated magnetic properties for different defect configurations of Co and O impurities in the ZnO wurtzite structure.

Model clusters	$S+O_V$ (xy)	$S+O_V$ (z)	$2S$	$S+I$	$2S+I$	$3S+I$
$m_{Co(S)}$, μ_B	2.07	2.09	2.12	2.36	2.35	2.29
$m_{Co(I)}$, μ_B				1.23	1.25	1.31
$J_{Co(S)\text{-}Co(S)}$, meV			2 (AFM)		9 (AFM)	1 (FM)
$J_{Co(S)\text{-}Co(I)}$, meV				35 (FM)	28 (FM)	21 (FM)
T_C, K				381	497	773

Fig. 6(a): one is created by removing one of three O atoms in the xy plane $O_V(xy)$ and the other by removing an O atom in the z direction $O_V(z)$. The unoccupied O $2p$ PDOS of a cluster containing one Co(S) successfully reproduces the spectral features a through e appearing in the O $1s$ XAS spectra shown in Fig. 3. One can clearly see that the presence of O_V near the Co impurity atom practically does not influence the occupancy of electronic states at the bottom of the conduction band while it decreases spectral feature a and broadens feature b.

The effect of Co interstitials on the O $2p$ PDOS is also investigated by considering the clusters with two Co(S) atoms combined with one Co(I) and three Co(S) atoms with Co(I) and are shown as clusters (c) and (d) in Fig. 6, respectively. Both clusters containing Co(I) impurities show an enhanced spectral weight of peak a_1 and an onset of O $2p$ conduction band that shifts toward lower energy as the Co(S) concentration increases. This behavior is in reasonable agreement with experimental O $1s$ XAS spectra and thus reflects that the differences in O $1s$ XAS spectra of Co-doped ZnO samples and undoped ZnO (shown in Fig. 3) cannot be attributed to the presence of O_V defects but to the involvement of Co interstitials. This is also supported by observing reduced features d and e in our samples. As shown in Fig. 7, the O_V defects do not change features d and e while they are reduced when adding the Co(I) defects to ZnO clusters.

The spectral results and theoretical analysis reveal that our samples contain the Co(S) and Co(I) defects but the effect of these defects on the magnetic properties is still uncertain. That is why we have calculated the magnetic moments (m) and exchange interactions (J) for different configurations of Co defects and O_V using a method reported by Anisimov *et al.*[18] The values of T_C for corresponding defect configurations were also determined using a standard formula for the Ising model. The obtained magnetic properties are presented in Table I. According to the calculations, the exchange interaction between Co(S) atoms is rather weak and thus the cluster that only contains Co(S) defects is antiferromagnetic (AFM). In the case of the configurations containing both Co(S) and Co(I) defects, a ferromagnetic coupling (FM) can be induced through an exchange interaction between Co(S) and Co(I) atoms and the ferromagnetic ordering temperatures are well above RT.

As discussed earlier, the enhanced spectral weight (feature a_1 in Fig. 5) at the bottom of the O $2p$ conduction band apparently relates to the presence of Co interstitials, and the Co $L_{2,3}$ RIXS spectra do not exhibit any evidence for direct interaction between Co ions. The reasonable conclusion from these results is that the minority Co(I) defects are isolated from the majority Co(S) atoms and thus do not participate in cluster formation. This absence of Co(S)-Co(I) exchange interaction in our samples explains why they do not exhibit ferromagnetic behavior.[9] In order to confirm this estimation, we superimpose the x-ray emission spectra of the constituent elements in Fig. 8. The resulting spectrum corresponds to the total density of valence states of the $Zn_{0.90}Co_{0.10}O$ sample. Note that the resonant Co $L_{2,3}$ XES spectrum taken at the L_2 edge is chosen for this comparison because it is less affected by self-absorption effects (than the spectra excited at the L_3 edge). To convert the emission energies of each spectrum to the binding energy scale relative to the Fermi level, we used Co $2p_{1/2}$, Zn $2p_{3/2}$, and O $1s$ binding energies for $Zn_{0.95}Co_{0.05}O$ thin film previously determined by x-ray photoemission spectroscopy.[19] As shown in Fig. 8, the Zn $3d$ states reside at the bottom of the valence band and slightly hybridize with O $2p$ states, which are mostly concentrated in the middle of the valence band. Co $3d$ states prevail in the region near the Fermi level. The energy difference between the valence centers of Co $3d$ and O $2p$ states is 1.67 eV. This energy separation between Co $3d$ and O $2p$ states is compared to DOS calculations for the clusters containing Co(S) and Co(I) defects shown in Fig. 9. The increase in Co(S) concentration does not change the relative energy position between Co and O valence states and their energy separation is about 1.7 eV, while the cluster containing both Co(S) and Co(I) has a wider separation of about 2.4 eV. From this com-

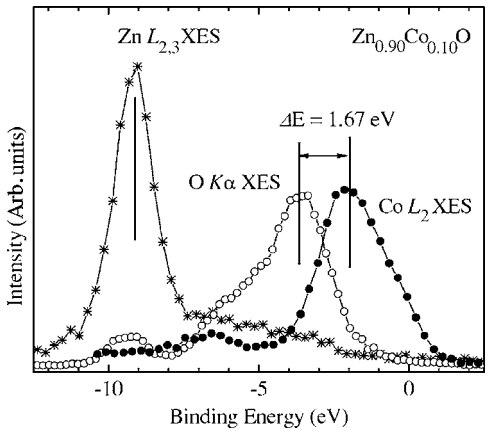

FIG. 8. Superposed XES spectra of Zn, Co, and O in the $Zn_{0.90}Co_{0.10}O$ sample. All spectra are plotted on the common binding energy scale.

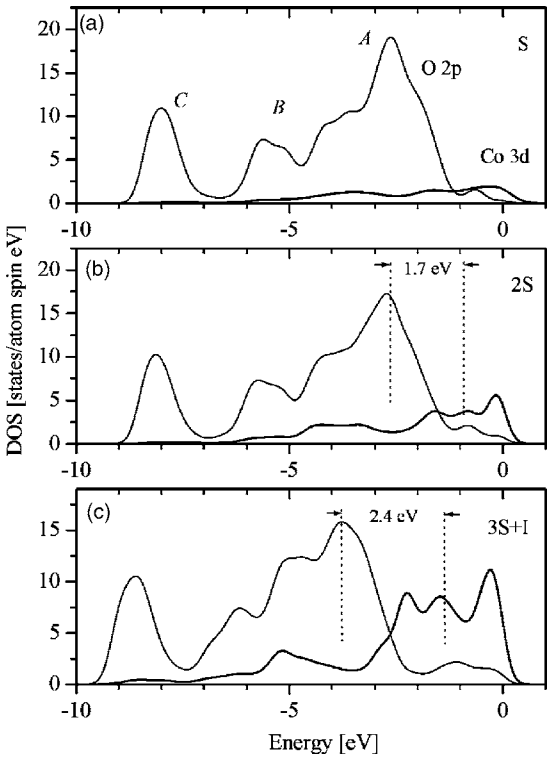

FIG. 9. Calculated DOS of occupied Co 3*d* and O 2*p* states with *S*, 2*S*, and 3*S*+*I* model configurations. The vertical lines are given to guide the eye when comparing experimental spectra and roughly show the main peak of O 2*p* and the center of gravity of Co 3*d* states.

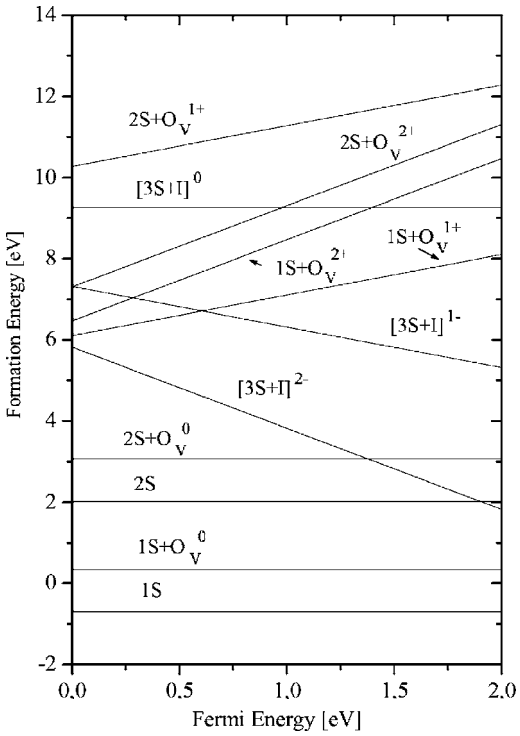

FIG. 10. Defect-formation energies as a function of the Fermi energy.

parison we conclude that the excess Co interstitials in $Zn_{0.90}Co_{0.10}O$ do not participate in cluster formation.

Finally, the defect-formation energies (E_{form}) for different cluster configurations are obtained by calculating total energies of the supercells based on a method described in Refs. 20 and 21. Since the defect-formation energies of a compound system depend on the atomic chemical potential (μ), the formation energy for a defect in a charge state q can be written as[20]

$$E_{form}(q) = E_T(q) - n_{Zn}\mu_{Zn} - n_O\mu_O - n_{Co}\mu_{Co} + qE_F, \quad (1)$$

where $E_T(q)$ is the total energy of the supercell with a defect in charge state q. In this notation, n_{Zn} (n_{Co} and n_O) stands for the number of Zn (Co and O) atoms in the supercell, μ_{Zn} (μ_{Co} and μ_O) is the atomic chemical potential, and E_F is the Fermi energy. We have used a Zn-rich limit (more favorable for O_V formation) where $\mu_O = \mu_{ZnO} - \mu_{Zn}$ and μ_{Zn} is the calculated chemical potential for the bulk Zn structure ($P63/mmc$). All calculations are performed using the SIESTA pseudopotential code because this method allows optimizing the atomic positions, and this optimization is required to take into account the correct calculation of E_{form}.[22]

The formation energies obtained for a Zn-rich limit are presented in Fig. 10 and show that the Co(*S*)-only configurations (1*S* and 2*S*) and those with neutral O_V defects ($S+O_V^0$ and $2S+O_V^0$) are the most likely ones to be formed (e.g., have the lowest formation energies) with respect to other charged configurations. However, those neutral O_V defects do not provide free charge carriers. In the case of the clusters with charged O_V defects ($1S+O_V^{1+}$, $2S+O_V^{1+}$, and $2S+O_V^{2+}$), which provide free carriers, the formation energies are almost two times higher than for configurations with neutral defects and are comparable to those containing both, Co(*S*) and Co(*I*) defects. These results suggest that it would be difficult to achieve ferromagnetic properties in $Zn_{1-x}Co_xO$ samples that are synthesized using a chemical-equilibrium method such as chemical precipitation and postannealing with respect to nonequilibrium epitaxial growth techniques.

IV. CONCLUSION

To conclude, we have investigated the electronic structure of Co-doped ZnO (with 2, 6, and 10 at. % of Co concentration) using soft x-ray spectroscopy and first principle calculations. The results reveal that Co dopants most likely substitute for Zn atoms and that free charge carriers are absent for a wide range of Co concentrations. The reason for this is that formation of interstitial Co impurities and charged oxygen vacancies is energetically less favorable than the formation of substitutional Co atoms. Our first-principles calculations suggest that high-T_C ferromagnetism in the Co-doped ZnO system requires not only free charge carriers to mediate the exchange interaction but also the interaction between substitutional and interstitial Co atoms through a cluster formation.

ACKNOWLEDGMENTS

This work is supported by the Natural Sciences and Engineering Research Council of Canada (NSERC) and the Canada Research Chair program. We gratefully acknowledge the Research Council of the President of the Russian Federation (Grants No. NSH-4192.2006.2 and NSH-4640.2006.2), and the Russian Science Foundation for Basic Research (Projects No. 05-02-16438 and 05-02-17704). The Advanced Light Source is supported by the Director, Office of Science, Office of Basic Energy Sciences, of the U.S. Department of Energy under Contract No. DE-AC02-05CH11231. D. W. Boukhvalov acknowledges support from Stichting voor Fundamenteel Onderzoek der Materie (FOM).

*Corresponding author. E-mail address: gapsoo.chang@usask.ca

[1] M. Rebien, W. Henrion, M. Bär, and Ch.-H. Fischer, Appl. Phys. Lett. **80**, 3518 (2002).
[2] K. Sato and H. Katayama-Yoshida, Jpn. J. Appl. Phys., Part 2 **39**, L555 (2000).
[3] F. Jalbout, H. Chen, and S. L. Whittenburg, Appl. Phys. Lett. **81**, 2217 (2002).
[4] K. Ueda, H. Tabata, and T. Kawai, Appl. Phys. Lett. **79**, 988 (2001).
[5] R. Janisch, P. Gopal, and N. A. Spaldin, J. Phys.: Condens. Matter **17**, R657 (2005), and references therein.
[6] Z. Jin, T. Fukumura, M. Kawasaki, K. Ando, H. Saito, T. Sekiguchi, Y. Z. Yoo, M. Murakami, Y. Matsumoto, T. Hasegawa, and H. Koinuma, Appl. Phys. Lett. **78**, 3824 (2001).
[7] D. P. Norton, M. E. Overberg, S. J. Pearton, K. Pruessner, J. D. Budai, L. A. Boatner, M. F. Chisholm, J. S. Lee, Z. G. Khim, Y. D. Park, and R. G. Wilson, Appl. Phys. Lett. **83**, 5488 (2003).
[8] A. S. Risbud, N. A. Spaldin, Z. Q. Chen, S. Stemmer, and R. Seshadri, Phys. Rev. B **68**, 205202 (2003).
[9] M. Bouloudenine, N. Viart, S. Colis, J. Kortus, and A. Dinia, Appl. Phys. Lett. **87**, 052501 (2005).
[10] J. Okabayashi, K. Ono, M. Mizuguchi, M. Oshima, S. S. Gupta, D. D. Sarma, T. Mizokawa, A. Fujimori, M. Yuri, C. T. Chen, T. Fukumura, M. Kawasaki, and H. Koinuma, J. Appl. Phys. **95**, 3573 (2004).
[11] S. Krishnamurthy, C. McGuinness, L. S. Dorneles, M. Venkatesan, J. M. D. Coey, K. E. Smith, T. Learmonth, P.-A. Glans, and J.-H. Guo, J. Appl. Phys. **99**, 08M111 (2006).
[12] N. A. Spaldin, Phys. Rev. B **69**, 125201 (2004).
[13] S. M. Butorin, J. Electron Spectrosc. Relat. Phenom. **110-111**, 213 (2000).
[14] E. Z. Kurmaev, A. L. Ankudinov, J. J. Rehr, L. D. Finkelstein, P. F. Karimov, and A. Moewes, J. Electron Spectrosc. Relat. Phenom. **148**, 1 (2005).
[15] G. S. Chang, E. Z. Kurmaev, D. W. Boukhvalov, L. D. Finkelstein, D. H. Kim, T.-W. Noh, A. Moewes, and T. A. Callcott, J. Phys.: Condens. Matter **18**, 4243 (2006).
[16] V. I. Grebennikov, Surf. Invest. X-Ray Synchrotron Neutron Tech. **11**, 41 (2002).
[17] O. K. Andersen, Phys. Rev. B **12**, 3060 (1975).
[18] V. I. Anisimov, F. Aryasetiawan, and A. I. Lichtenstein, J. Phys.: Condens. Matter **9**, 767 (1997).
[19] M. Kobayashi, Master thesis, Tokyo University, 2005.
[20] F. Oba, S. R. Nishitani, S. Isotani, and H. Adachi, J. Appl. Phys. **90**, 824 (2001).
[21] S. B. Zhang, S.-H. Wei, and A. Zunger, Phys. Rev. B **63**, 075205 (2001).
[22] J. M. Soler, E. Artacho, G. D. Gale, A. Garsia, J. Junquera, P. Ordejón, and D. Sánchez-Portal, J. Phys.: Condens. Matter **14**, 2745 (2002).